
Article:
Wei, C orcid.org/0000-0002-4565-509X, Romano, R orcid.org/0000-0002-2132-4077, Merat, N orcid.org/0000-0003-4140-9948 et al. (5 more authors) (2019) Risk-based autonomous vehicle motion control with considering human driver's behaviour. Transportation Research Part C: Emerging Technologies, 107. pp. 1-14. ISSN 0968-090X

https://doi.org/10.1016/j.trc.2019.08.003

Risk-based Autonomous Vehicle Motion Control with Considering Human Driver's Behaviour

Chongfeng Wei[1,*], Richard Romano[1], Natasha Merat[1], Yafei Wang[2], Chuan Hu[3], Hamid Taghavifar[4], Foroogh Hajiseyedjavadi[1], Erwin R. Boer[1]

[1]Institute for Transport Studies, University of Leeds, Leeds, UK

[2]School of Mechanical Engineering, Shanghai Jiao Tong University, Shanghai, China

[3]Department of Mechanical Engineering University of Texas at Austin, Austin, Texas, US

[4]Department of Mechanical Engineering, Concordia University, Canada

[*]Corresponding author:

Chongfeng Wei, weichongfeng@gmail.com, c.wei2@leeds.ac.uk

Abstract: The selected motions of autonomous vehicles (AVs) are subject to the constraints from the surrounding traffic environment, infrastructure and the vehicle's dynamic capabilities. Normally, the motion control of the vehicle is composed of trajectory planning and trajectory following according to the surrounding risk factors, the vehicles' capabilities as well as tyre/road interaction situations. However, pure trajectory following with a unique path may make the motion control of the vehicle be too careful and cautious with a large amount of steering effort. To follow a planned trajectory, the AVs with the traditional path-following control algorithms will correct their states even if the vehicles have only a slight deviation from the desired path or the vehicle detects static infrastructure like roadside trees. In this case, the safety of the AVs can be guaranteed to some degree, but the comfort and sense of hazards for the drivers are ignored, and sometimes the AVs have unusual motion behaviours which may not be acceptable to other road users. To solve this problem, this study aims to develop a safety corridor-based vehicle motion control approach by investigating human-driven vehicle behaviour and the vehicle's dynamic capabilities. The safety corridor is derived by the manoeuvring action feedback of actual drivers as collected in a driving simulator when presented with surrounding risk elements and enables the AVs to have safe trajectories within it. A corridor-based Nonlinear Model Predictive Control (NMPC) has been developed which controls the vehicle state to achieve a smooth and comfortable trajectory while applying trajectory constraints using the safety corridor. The safety corridor and motion controller are assessed using four typical scenarios to show that the vehicle has a human-like or human-oriented behaviour which is expected to be more acceptable for both drivers and other road users.

Keywords: Risk-based corridor, Autonomous Vehicles, Model Predictive Control, trajectory, Human-like

1. Introduction

Vehicle motion planning and trajectory following for automated vehicles is subject to the vehicle dynamic performance, surrounding environments, and road surface conditions. The risk factors resulting from the static and dynamic elements include the surrounding infrastructure and the dynamic properties of other road users. Current approaches of the vehicle's control and execution are to plan the motions of the vehicles with the detected road information and follow the desired trajectories. The safety aspect of AVs has been greatly focused on avoiding static obstacles, moving pedestrians and other road vehicles when the sensor system has detected the relevant surrounding environment. However, comfort and reliability of the vehicles should not be ignored as they are also important for the future development of AVs because of their benefits for the drivers and other road users. Existing motion planning and trajectory following algorithms rarely consider the comfort and sense of security and confidence for the drivers and passengers in the AVs, which may lead to a nervous experience for them. Pure motion planning and trajectory following may make the behaviour of the AVs be unusual and confused for other human-driven vehicles and other road users, and thus lead to traffic jams and accidents. Therefore, it is necessary and urgent to rethink and reconsider the motion planning and trajectory following solutions.

For vehicle motion control algorithm development, one of the most important factors to be considered is the vehicle's own capability. Substantial research has been conducted on motion planning and trajectory tracking for robots and unmanned aerial vehicles, but the vehicles' motion planning and execution is still a challenge because of the lack of consideration of the vehicle dynamic capacities and varying environment elements. A vehicle's motion capacity is not only limited by the external environment, but also determined by the vehicle's dynamic capabilities such as stability requirement, electrical control system characteristics, and tyre/road interaction adhesion capability, which is dynamically changing in different road surfaces.

The motion planning models for road vehicles are normally developed on the basis of the path planning in mobile robotics and modified with consideration of the challenges of road information and driving rules. As one of the path planning techniques, a collision avoidance system is used to generate a desired trajectory to avoid obstacles by considering the spatial and geometric characteristics of the obstacles as well as the mobile robots' kinematic properties (Rashid et al., 2013). According to the implementation of the motion planning techniques in autonomous driving, the planning approaches can be classified into four categories: Graph search based plan (Ferguson et al., 2008; Kala and Warwick, 2013), Sampling based plan (Jeong hwan et al., 2013; Karaman et al., 2011; Kuwata et al., 2009), Interpolating curve plan (Berglund et al., 2010; Chu et al., 2012; González et al., 2014; Wenda et al., 2012) and numerical optimization approach (Ziegler et al., 2014). To involve the vehicle constraints, speed and comfort elements, recent demonstrations have used optimal polynomial curves in terms of smoothness to deal with real implementations (González et al., 2016). However, due to the complex and fluctuating dynamic environment elements such as pedestrians, cyclists and other vehicles, collision free trajectory generation within a limited time is still a challenge. Moreover, multiple constraints ranging from the vehicle dynamic limitations and passengers' comfort are necessary and challenging for the vehicle motion planning to generate smooth and achievable trajectories (González et al., 2016).

Vehicle dynamic properties particular for tyre/road interaction situation are normally considered as one of the vehicle kinematic properties. Due to the varying road conditions such

as road unevenness and friction coefficient, the vehicle's stability limitations and adhesion limitation will be changing in real time and make the vehicle motion planning more challenging. To make sure the vehicle can have a smooth motion, some objectives such as minimization of acceleration or jerk is normally considered by using trajectory polynomial, but tyre/road interaction variation effect on the longitudinal and lateral behaviour of vehicles are ignored frequently in order to simplify the calculation of the trajectory planning (Ntousakis et al., 2016). These simplifications may make the applicability and feasibility of the path following to be limited. In the past decades, many tyre models have been developed for model-based design and vehicle controller design (Wei et al., 2016; Wei et al., 2017). The friction coefficient, the lateral velocity of the vehicle and the vertical load affect the lateral tyre force, and the linear district of the tyre/road interaction are varying for different road types (Du et al., 2011; Wei and Olatunbosun, 2016). To simplify the vehicle motion control with complex tyre/road interaction and guarantee the vehicle's stability, the tyre slip angle is normally limited into its linear range (Ji et al., 2017).

For the trajectory or path tracking of AVs or mobile robots, the commonly used methods are sliding-mode control (Hu et al., 2016b), robust control (Hu et al., 2016a) and fuzzy logic (Antonelli et al., 2007). However, many of the vehicles' dynamic limitations, particularly nonlinear characteristics, have been ignored in these controllers to simplify the vehicle control system and increase the efficiency of calculation (Ji et al., 2017). Moreover, pure path tracking of AVs rarely consider the drivers' or other road users' sense of risk elements. The drivers in the AVs not only want the vehicles to avoid the collisions but also keep a suitable distance from the risk elements even if the risk element is a road kerb or grass. Due to the uncertainties during the vehicle control, even the straight road has the potential to lead to a collision between the vehicle and the road edge. Boer (Boer, 2016) proposed a theoretical time to line crossing (TLC) model to capture the risk for both straight road and curved road as a function of environment and driver skill factors, and the drivers' lateral offset tolerance were analytically obtained. Boer's model demonstrates that it is necessary to consider the drivers' sense of security and confidence during vehicle motion control.

A new approach to vehicle motion planning and trajectory tracking is to involve the human driver into the procedure. Compared to the robotic calculation of the planned trajectory, human-driven vehicles follow a trajectory that is planned by considering the drivers and the passengers' feelings, including both the physiological comfort and the psychological comfort. However, it is difficult to realize this with a unique planned path due to the complexity of human drivers' behaviour, and few driver models within the motion planning and trajectory following have quantitatively considered driver behaviour (Wu et al., 2014). Gu et al. (Gu et al., 2016) developed a human-like planning approach that is capable of learning passengers' individual driving styles, but it demonstrated a relatively large behaviour discrepancy due to the lack of human driver properties stochastics. Drivers' volition in terms of time to line crossing and time to collision, for both straight road and curved road, affect main factors that affect the risk levels assessed by drivers or passengers (Wu et al., 2014).

Therefore, to plan the vehicles' motion, like a human-driver, requires the identification of characteristics of natural driving and risk factors which influence driver behaviour. The human drivers' may have an imaginary trajectory planned by themselves during their driving, but they will not attempt to shrink the error between the vehicles' states and the planned trajectory as long as the vehicles' states are limited to a safe and comfortable environment, which is different from the traditional path following approaches. The traditional path following approach always

tends to correct the error between the planned trajectory and the vehicles' current states, which make the autonomous driving of the vehicles be unusual and too cautious. For the human-driven vehicles, when the vehicles deviate from the drivers' imaginary trajectory because of the uncertainties of vehicle system or the road, the drivers normally keep the vehicles' status at that moment and choose another suitable trajectory. This means a flexible space of available trajectories is needed for AVs if we consider the sense of the drivers, and the AVs' movement can be limited to the space that avoids the potential risk elements.

To this end, this study aims to build a risk-based corridor, rather than planning a unique path, based on the environmental risk elements and the vehicle's dynamic properties, where drivers' behaviour are considered. Within the corridor, vehicle motion control algorithms are developed to make sure the AVs can provide a smooth and comfortable movement for the drivers. As a dynamic optimization control algorithm, Model Predictive Control (MPC) is an advantageous approach for dealing with nonlinear dynamic problems with multiple constraints. Moreover, one of the characteristics of MPC is rolling-horizon optimization, so it can overcome the influence of environment disturbances. Considering the vehicles' nonlinear dynamics and human drivers' sense of confidence, this study develops a Nonlinear Model Predictive Control (NMPC) algorithm to make the autonomous driving of the vehicles be more comfortable and natural.

2. Human-like vehicle control framework

The proposed human-like control algorithm aims to develop a vehicle dynamic controller on the basis of human driver behaviour when interacting with environment risks. The framework of the control algorithm is shown in Figure 1. When the road information has been detected, the human driver will react to the existing and potential risks through modifying the steer angle and the speed of the vehicle. By testing different driver behaviour for the same road information, it is able to conduct an estimation of the range of the speeds, lateral offset, gaps, and vehicle's heading angle and acceleration that drivers can accept around environment elements in the scene. Hence, a risk-based corridor (or risk model) is established to restrict the vehicle's motion. The risk-based corridor due to the environmental risk elements can be constraints on vehicle velocity, lateral offset and yaw rate etc. It is noted that the risk-based corridor is not only determined by the road information directly but also determined by the sense of the drivers in AVs. Therefore, the corridor can be derived by the investigation of the drivers' manoeuvring actions, i.e. speed control, steering angle and steering speed control, when detecting the environmental risk elements such as obstacles, road edges, and other road vehicles. With the derived corridor, the safety and sense of security for the drivers or the passengers can be guaranteed by setting the corresponding constraints.

Another corridor that is necessary to be considered is the envelope of the vehicle's dynamic characteristics. Due to the complex properties of the interaction between tyre and road, many studies have been carried out to investigate the nonlinear properties of the tyre, particularly on severe conditions. The constraints, for the vehicle dynamic controller, not only include the risk factors because of the road information, but also the vehicles' kinematic capabilities and tyre/road interaction limitations. The primary objective of AVs is to guarantee safety which is normally initially ensured by staying within the vehicle's stability and tyre/road adhesion envelop. Both the longitudinal and lateral motions of the vehicle are subject to the tyre/road interaction and they affect each other. Moreover, as a mechanical system with an active control chassis, the vehicle's motion is also limited by the mechanical properties and electrical control

system characteristics. Thus, the definition of the envelope of vehicle dynamic properties is necessary to guarantee the vehicle's stability.

Within the risk-based corridor and vehicle dynamic corridor, the vehicle's motion can be limited to a safety horizon. To have a natural and comfortable driving feeling for the passengers, the human drivers may expect the vehicle motion be smooth and relaxed, which means the vehicle states variation should not be large while the perception and reaction to static and dynamic risk elements should be appropriate. Hence, the human-driver's behaviour is also used to optimize the vehicle kinematic behaviour to guarantee a natural feeling of driving.

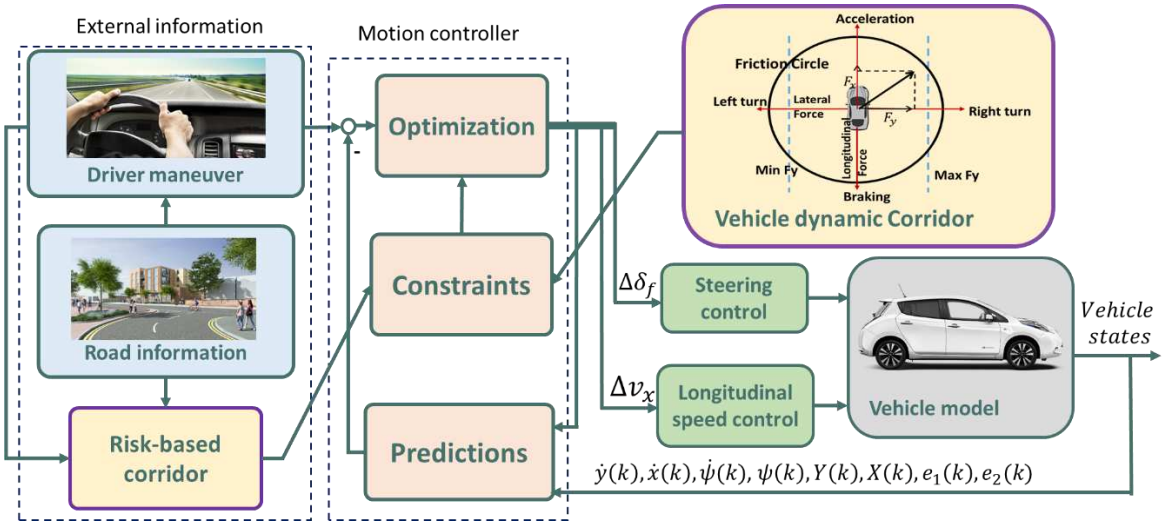

Figure 1 Framework of human-like control algorithm

3. Risk-based lateral offset boundary generation

The safety corridor is based on the analysis of interactions between human drivers and different road environments including the straight and curved roads with grass or kerbs at the roadside, obstacles like parked cars and pedestrians outside or inside the road, and other moving vehicles. With the perception of the environmental risk elements, a virtual risk boundary in terms of acceptable lateral offset, speed and yaw rate can be generated according to the drivers' action feedbacks and the risk levels of the environment elements, as shown in Figure 2. It is not difficult to understand that the walking pedestrian at the side of the road produces a higher level of perceived risk by the driver than the trees located at the side of the road, so the lateral gap between the risk boundary and the kerb for the pedestrian should be larger than that for the tree. The lateral position boundary (risk boundary in *Figure 2*) for the AV moving is just one of the factors to form the risk-based corridor, and it also includes the lateral acceleration range, the longitudinal velocity variation range and the vehicle's yaw angle limitation. These factors can be well derived through the measurement of the human drivers' behaviour using a driving simulator. In this way, a risk-based corridor can be generated as a function of the longitudinal position on the path, the lateral offset, the longitudinal velocity and acceleration and the yaw angle of the vehicle. In this study, only acceptable lateral offsets are used for the following vehicle motion controller development, and other vehicle states tolerance derivation will be investigated and considered in future studies.

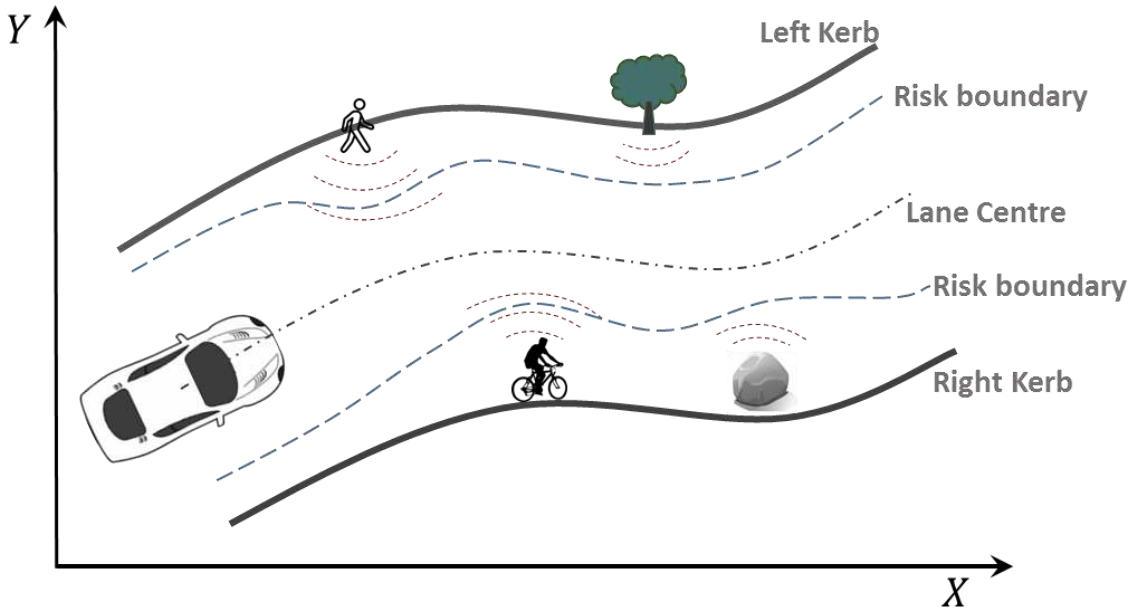

Figure 2 The generation of the risk-based corridor

The University of Leeds Driving Simulator (UoLDS, *Figure 3*) was employed to evaluate the effect of the perception of environmental risk elements on driving performance, and thus the derivation of the risk-based tolerance such as acceptable lateral offset and desired speed. The simulator system collects data ranging from the vehicle states (position, speed, acceleration, etc.) that result from the drivers' performance, other AVs' states in the scene and other data relating to drivers' behaviour.

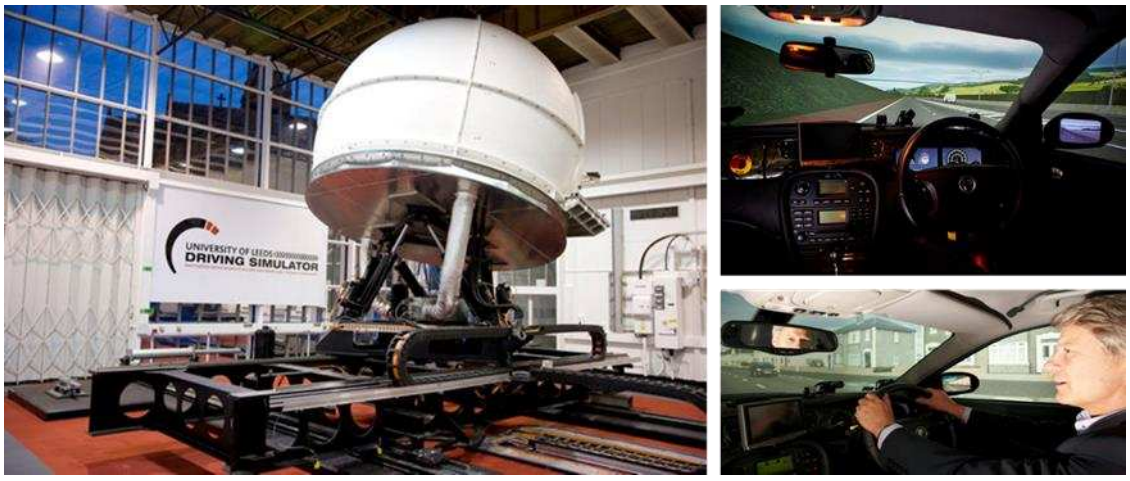

Figure 3 Illustration of the driver simulator for collecting driving data of vehicles and drivers

A total of 44 participants between the age of 18 to 65 years participated in the driving simulation experiment. Each subject drove all of the designed scenarios which involved different roadway environments, roadway geometry, roadside context, and traffic condition. Participants also drove a 20-minute practice drive before the two 40-45 minutes sessions during which data was collected. The purpose of the practice drive was for the participants to get familiar with the simulator and the driving environment.

The vehicle data was collected at 60 Hz and included the speed and lateral position of the vehicle. The offset from the centre of the travel lane is calculated from the lateral position at each time step and is aggregated for all the drivers for each road segment with a constant risk (i.e. specific roadway environment, roadside context, roadway geometry, and traffic condition). Four different road conditions were tested and the lateral offset data of the vehicles for these scenarios were collected and are shown in Figure 4. The 5th and 95th percentile of the lateral offset is then calculated for each segment and is assumed as the left most and right most edge of the comfortable driving corridor for the average drivers. This corridor is assumed to have the acceptable risk for the average drivers. In other words, any point on the roadway that is outside this corridor is assumed to have a risk level higher than the acceptable risk threshold and is not accepted by the average of the drivers. The derived acceptable lateral offsets for different road types are illustrated in

Table ***1***. With the derived risk-based lateral offset tolerance for the typical road types, the constraint in terms of lateral offset for the curved road with the similar radius and roadside can be obtained by finding the corresponding acceptable lateral offsets.

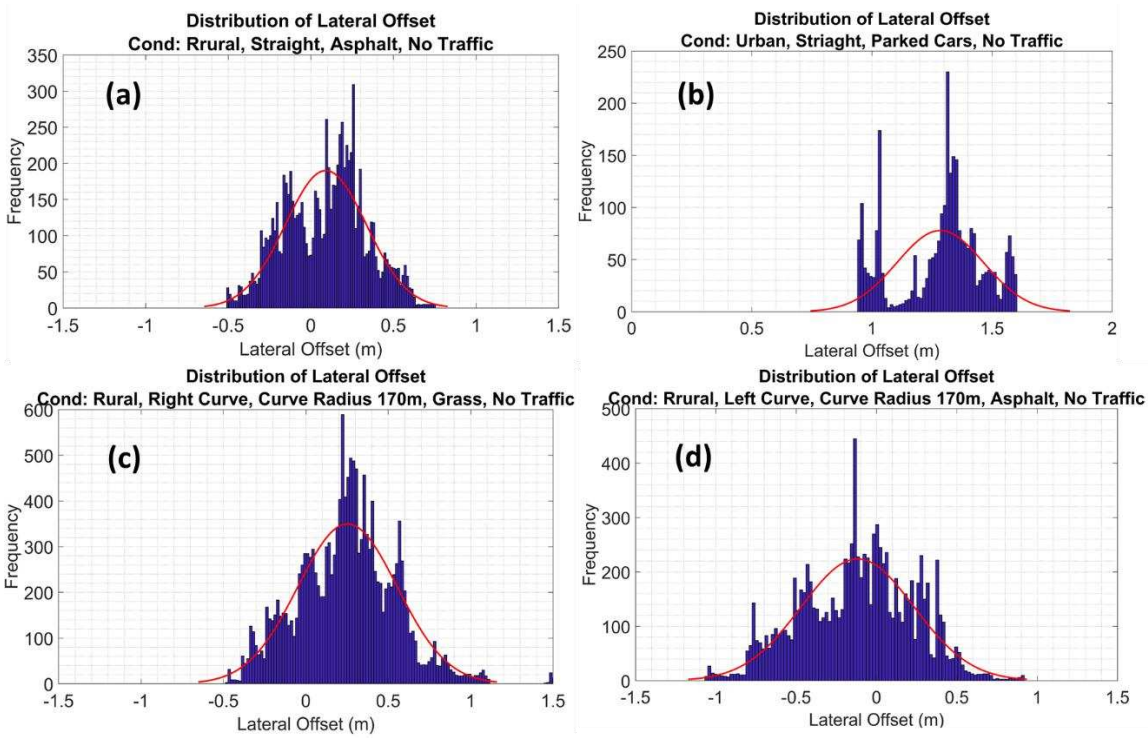

Figure 4 Distribution of measured vehicle lateral offsets for different drivers at the scenarios: a) straight asphalt road, b) straight road with parked cars at the roadside, c) Right curve road with a radius of 170 m and grass at the side of the road d) Left curve road with a radius of 170 m and asphalt at the side of the road

Table 1 Derived acceptable lateral offset at different scenarios based on the driving tests

risk code	5% offset from centre of lane (m)	95% offset from centre of lane (m)	environment	curve radius (m)	curve direction	roadside
1020010	-0.7327	0.4138	'rural'	'170'	'curve-left'	'asphalt'
1021020	-0.2342	0.7492	'rural'	'170'	'curve-right'	'grass'
1000000	-0.2983	0.5017	'rural'	'straight'	'straight'	'asphalt'
2004000	0.9889	1.9695	'urban'	'straight'	'straight'	'blockage'

4. Vehicle dynamic model for the MPC

In this study, the vehicle dynamic model used for controller design is simplified to a kinematic bicycle model which is normally used for vehicle motion planning and path tracking as the suspension movement and rolling resistance influences are neglected. Figure 5 shows the kinematic bicycle model in the global coordinate system and the deviation description relative to the road centre line path. We use the distance between the road centre line and the C.G. of the vehicle to define the deviation of the vehicle on the path, as shown in Figure 5(b).

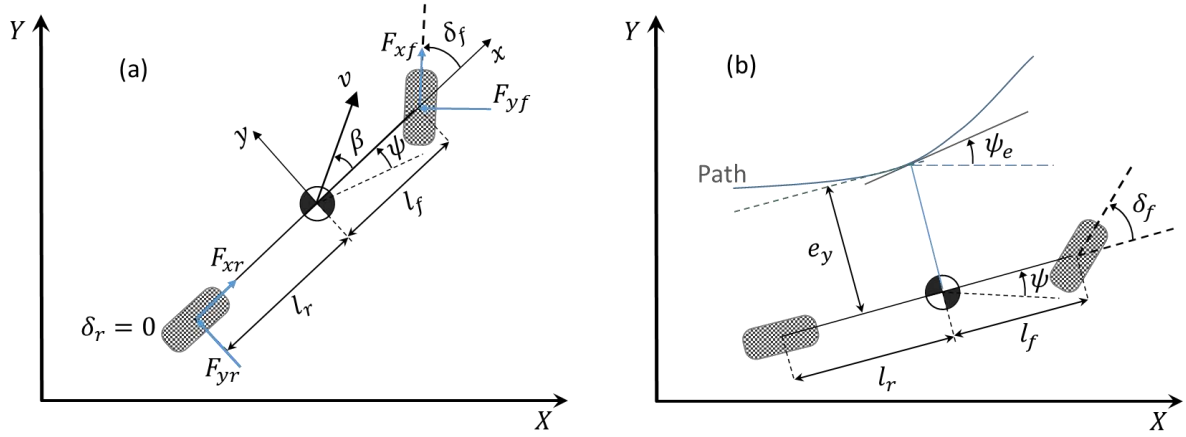

Figure 5 Simplified vehicle dynamic model for system prediction within MPC: (a) kinematic bicycle model in the global coordinate system, (b) kinematic bicycle model to describe the path deviation

In this case, the differential equations of the vehicle's motion in terms of lateral movement y, longitudinal movement x, yaw rate of the vehicle body $\dot{\psi}$ and orthogonal distance e_y, the difference between the heading angle of the road and the heading angle of the vehicle e_ψ can be given as

$$\ddot{y} = -\dot{x}\dot{\psi} + \frac{2}{m}\left(F_{yf}\cos\delta_f - F_{xf}\sin\delta_f + F_{yr}\right) \tag{1}$$

$$\ddot{x} = \dot{y}\dot{\psi} + \frac{2}{m}\left(F_{xf}\cos\delta_f - F_{yf}\sin\delta_f + F_{xr}\right) \tag{2}$$

$$\ddot{\psi} = \frac{2}{I_z}\left(l_f\left(F_{yf}\cos\delta_f + F_{xf}\sin\delta_f\right) - l_r F_{yr}\right) \tag{3}$$

$$\dot{X} = \dot{x}\cos\psi - \dot{y}\sin\psi \tag{4}$$

$$\dot{Y} = \dot{x}\sin\psi + \dot{y}\cos\psi \tag{5}$$

$$\dot{e}_y = \dot{y} + \dot{x}e_\psi \tag{6}$$

$$\dot{e}_\psi = \dot{\psi} - \frac{\dot{x}}{R} \tag{7}$$

where R is the curve radius in real time, and it is set to 9999 for a straight road. I_z and m represent the vehicle's yaw inertia and mass, respectively. $\dot{x}$ and $\dot{y}$ denote the longitudinal and lateral speeds in the body frame and $\dot{\psi}$ denotes the yaw rate. F_{yf} , F_{xf}, F_{yr} and F_{xr} represent the lateral and longitudinal tyre forces at the front and rear wheels, in coordinate frames aligned with the wheels. The slip angle of the front and rear tyre is given as

$$\alpha_f = \tan^{-1}\left(\frac{\dot{y} + l_f\dot{\psi}}{\dot{x}}\right) - \delta_f \tag{8}$$

$$\alpha_r = \tan^{-1}\left(\frac{\dot{y} - l_r\dot{\psi}}{\dot{x}}\right) \tag{9}$$

For small tyre slip angles, the lateral tyre forces are normally defined as linearly proportional to the slip angle, which can be expressed as

$$F_{yf} = -c_f\alpha_f \tag{10}$$

$$F_{yr} = -c_r\alpha_r \tag{11}$$

The generation of the road can be conducted with the curvature of the road ρ at any distance, and the heading of the road at the corresponding distance position. The heading of the road ψ_e and the global coordinate $[X_r, Y_r]$ along the path can be derived by

$$\psi_e(s) = \int_0^s \rho(\lambda)\mathrm{d}\lambda + \psi_{e0} \tag{12}$$

$$X_r(s) = \int_0^s \cos[\psi_e(s)]\mathrm{d}\lambda + X_{r0} \tag{13}$$

$$Y_r(s) = \int_0^s \sin[\psi_e(s)]\mathrm{d}\lambda + Y_{r0} \tag{14}$$

where ψ_{e0} and $[X_{r0}, Y_{r0}]$ are the initial heading and position of the road curve in the globe coordinate system.

Selecting global lateral position, longitudinal position, yaw angle, yaw rate, vehicle lateral deviation as output, state space equation of the system can be expressed as

$$\dot{X}_s = A(t)X_s + B(t)u \tag{15}$$

$$Y_s = CX_s \tag{16}$$

where $X_s = [\dot{y}, \dot{x}, \psi, \dot{\psi}, Y, X, e_y, e_\psi]^{\mathrm{T}}$, $Y_s = [\dot{y}, \dot{\psi}, e_y, e_\psi]^{\mathrm{T}}, u = \delta_f$

$$A=\begin{bmatrix}
\frac{-2\left(C_{cf}+C_{cr}\right)}{m\dot{x}} & \frac{\left(2C_{cf}\left(\dot{y}+a\dot{\psi}\right)+2C_{cr}\left(\dot{y}-b\dot{\psi}\right)\right)}{m\dot{x}^2}-\dot{\psi} & 0 & -\dot{x}+\frac{2\left(bC_{cr}-aC_{cf}\right)}{m\dot{x}} & 0 & 0 & 0 & 0\\
\varphi-\frac{2C_{cf}\delta_f}{m\dot{x}} & \frac{\left(2C_{cf}\delta_f\left(\dot{y}+a\dot{\psi}\right)\right)}{m\dot{x}^2} & 0 & \dot{y}-\frac{2aC_{cf}\delta_f}{m\dot{x}} & 0 & 0 & 0 & 0\\
0 & 0 & 0 & 1 & 0 & 0 & 0 & 0\\
\frac{2\left(bC_{cr}-aC_{cf}\right)}{I_z\dot{x}} & \frac{\left(2C_{cf}\left(\dot{y}+a\dot{\psi}\right)+2C_{cr}\left(\dot{y}-b\dot{\psi}\right)\right)}{m\dot{x}^2} & 0 & \frac{-2\left(a^2C_{cf}+b^2C_{cr}\right)}{I_z\dot{x}} & 0 & 0 & 0 & 0\\
\cos\left(\psi\right) & \sin\left(\psi\right) & \dot{x}\cos\left(\psi\right)-\dot{y}\sin\left(\psi\right) & 0 & 0 & 0 & 0 & 0\\
-\sin\left(\psi\right) & \cos\left(\psi\right) & -\dot{y}\cos\left(\psi\right)-\dot{x}\sin\left(\psi\right) & 0 & 0 & 0 & 0 & 0\\
1 & e_{\psi} & 0 & 0 & 0 & 0 & 0 & \dot{x}\\
0 & -\frac{1}{R} & 0 & 1 & 0 & 0 & 0 & 0
\end{bmatrix}$$

$$B=\begin{bmatrix}
\frac{2C_{cf}}{m}\\
\frac{2C_{cf}\left(2\delta_f-\frac{\dot{y}+a\dot{\psi}}{\dot{x}}\right)}{m}\\
0\\
\frac{2aC_{cf}}{I_z}\\
0\\
0\\
0\\
0
\end{bmatrix},\quad C=\begin{bmatrix}
1 & 0 & 0 & 0 & 0 & 0 & 0 & 0\\
0 & 0 & 0 & 1 & 0 & 0 & 0 & 0\\
0 & 0 & 0 & 0 & 0 & 0 & 1 & 0\\
0 & 0 & 0 & 0 & 0 & 0 & 0 & 1
\end{bmatrix}. \tag{17}$$

It is noted that only the front steering angle is considered as the input in this model, and the velocity of the vehicle is kept constant in time domain. In this case, the longitudinal slip inputs can be ignored. The above state space equations of the vehicle system are continuous-time and cannot be used for the design of MPC algorithms directly. Thus, the model of the system is converted to a discrete state-space model by discretizing the state-space equations. The Euler method is used to discretize the state-space model with a sample time of T_s , then the system can be described in discrete form

$$X_d\left(k+1\right)=A_dX_d\left(k\right)+B_du\left(k\right) \tag{18}$$

$$Y_d\left(k\right)=C_dX_d\left(k\right) \tag{19}$$

where A_d, B_d and C_d are the discrete matrices for the state-space equation, respectively, which can be obtained by

$$A_d=e^{A(t)T_s} \tag{20}$$

$$B_d=\int_{kT_s}^{(k+1)T_s}e^{A(t)\left[(k+1)T_s-\tau\right]}B_d\mathrm{d}\tau \tag{21}$$

$$C_d=C=\begin{bmatrix}
1 & 0 & 0 & 0 & 0 & 0 & 0 & 0\\
0 & 0 & 0 & 1 & 0 & 0 & 0 & 0\\
0 & 0 & 0 & 0 & 0 & 0 & 1 & 0\\
0 & 0 & 0 & 0 & 0 & 0 & 0 & 1
\end{bmatrix} \tag{22}$$

5. Controller design

5.1 Prediction of vehicle states and output variables

One important property of MPC is receding horizon optimization, and the prediction of the vehicle's states and output variables is important to determine the control inputs within a specified horizon. Based on this prediction, the specified performance index at each time t is optimised under operating constraints in order for the optimal manoeuvring action inputs to be determined.

The first of such optimal action is the control input applied to the vehicle system at time k, and at time $k+1$, a new optimization is obtained over a shifted prediction horizon. The prediction horizon of the system is defined as N_p, and the control horizon is N_c, the state vector $X_p(k+i,k)$ and the control input vector $\Delta u(k+i,k)$ are replaced by $X_p(k+i)$ and $\Delta u(k+i,k)$ respectively. Thus, the vehicle states and the vehicle system's output variables in the prediction horizon can be calculated as follows:

$$\begin{aligned}
X_p(k+1) &= A_p^{(k)} X_p(k) + B_p \Delta u(k) \\
X_p(k+2) &= A_p^{(k+1)} A_p^{(k)} X_p(k) + A_p^{(k)} B_p \Delta u(k) + B_p \Delta u(k+1) \\
&\vdots \\
X_p(k+N_c) &= \prod_{i=0}^{N_c-1} A_p^{(k+i)} X_p(k) + \prod_{i=0}^{N_c-2} A_p^{(k+i)} B_p \Delta u(k) + \cdots + B_p \Delta u(k+N_c-1) \\
&\vdots \\
X_p(k+N_p) &= \prod_{i=0}^{N_p-1} A_p^{(k+i)} X_p(k) + \prod_{i=0}^{N_p-2} A_p^{(k+i)} B_p \Delta u(k) + \cdots + \prod_{i=0}^{N_p-N_c-1} A_p^{(k+i)} B_p \Delta u(k+N_c-1)
\end{aligned} \tag{23}$$

As in standard MPC schemes, the prediction horizon N_p is larger than the specified control horizon N_c, and it is assumed that the control inputs are kept constant for all $N_c \le k \le N_p$ i.e. $\Delta u(k+i) = 0,\ \forall\, i \ge N_c$. The sequence of the input increments derived at time k can be written as

$$\Delta U_k = [\Delta u(k), \Delta u(k+1), ..., \Delta u(k+N_c-1)]^{\mathrm{T}} \tag{24}$$

Therefore, the output vector predicted at time k can be expressed as

$$Y_p(k) = \Psi_p X_p(k) + \Theta_p \Delta U_k \tag{25}$$

in which

$$\Psi_p = \left[C_p A_p^{(k)}, C_p A_p^{(k+1)} A_p^{(k)}, ..., C_p \prod_{i=0}^{N_c-1} A_p^{(k+i)}, ..., C_p \prod_{i=0}^{N_p-1} A_p^{(k+i)} \right]^{\mathrm{T}} \tag{26}$$

and

$$\Theta_p = \begin{bmatrix} C_p B_p & 0 & \cdots & 0 \\ C_p A_p^{(k)} B_p & C_p B_p & 0 & 0 \\ \vdots & \vdots & \ddots & 0 \\ C_p \prod_{i=0}^{N_c-2} A_p^{(k+i)} B_p & C_p \prod_{i=0}^{N_c-3} A_p^{(k+i)} B_p & \cdots & C_p B_p \\ C_p \prod_{i=0}^{N_c-1} A_p^{(k+i)} B_p & C_p \prod_{i=0}^{N_c-2} A_p^{(k+i)} B_p & \cdots & C_p A_p^{(k)} B_p \\ \vdots & \vdots & \ddots & \vdots \\ C_p \prod_{i=0}^{N_p-2} A_p^{(k+i)} B_p & C_p \prod_{i=0}^{N_p-3} A_p^{(k+i)} B_p & \cdots & C_p \prod_{i=0}^{N_p-N_c-2} A_p^{(k+i)} B_p \end{bmatrix} \tag{27}$$

5.2 Optimization

The control input increments are derived through comparison between the desired vehicle motion parameters and the predicted output variables. At each time step, the controller solves a convex optimization problem to find an optimal sequence of increments of front steering angle input. Unlike the traditional optimal method, we don't want the vehicle's path to exactly follow a planned path or the lane centre line, in order that the cautious motion of the vehicle can be avoided. In this study, the design of the cost function is required to be able to guarantee the vehicle runs smoothly and comfortably within the lateral tolerance derived by the risk model. To this end, both vehicle states error relative to desired vehicle motion and the control input need to be optimized, and the cost function can be written as

$$\min_{\Delta U(t)} \; J(X_p(k), \Delta U(k)) = \sum_{i=1}^{N_p} \left\| Y_p(k+i) - Y_d(k+i) \right\|_Q^2 + \sum_{i=1}^{N_c-1} \| \Delta u_{k+i} \|_R^2 + \rho \varepsilon^2 \tag{28}$$

where the first summand reflects the desired performance on vehicle state tracking and the second is a measure of the steering effort. ρ represents the weight coefficient, ε is the relaxation factor and Q and R are weighting matrices of appropriate dimensions. Due to the complexity of the system and the multi-constraints, the involvement of a slack variable is needed and will avoid the circumstance that the system cannot get the optimal solution within the calculation time. In this study, the slack variable is associated to the tyre slip angles where soft constraints are defined to force the vehicle to operate within the linearity region of the tyre lateral dynamic behaviour.

To have a natural and comfortable driving experience for the drivers, we don't force the vehicle to exactly follow the centre line of the lane and the heading angle of the road. On the other hand, we allow the vehicle to have a more flexible motion within the obtained lateral offset corridor, and minimum yaw rate and minimum lateral velocity are taken as objects to optimise vehicle's comfortability, which align with human preference, i.e. they are not willing to yaw or move side to side frequently.

5.3 Vehicle dynamic constraints

To guarantee the vehicle's safety and stability, the safety corridor should consider the vehicle's dynamic performance and limit the vehicle's states into its dynamic envelop. This requires the application of the following constraints.

1. Vehicle stability

To guarantee the stability of the vehicle, it is necessary to apply constraints to the side-slip angle of the vehicle and the yaw rate. The limitation on the slip-angle is different for road surfaces with different adhesion characteristics, and the constraint for the side-slip angle is to prevent the vehicle approaching the adhesion limit. Similarly, it is also needed to constrain the yaw rate of the vehicle to stay in a safe range of the vehicle's dynamic states. Hence, the constraints of the side-slip angle and the yaw rate of the vehicle can be expressed as

$$\gamma_{\max} \le \gamma_{k+i,t} \le \gamma_{\min} \tag{29}$$

$$\beta_{\max} \le \beta_{k+i,t} \le \beta_{\min} \tag{30}$$

2. Vehicle's adhesion

Due to the tyre/road adhesion capability, the vehicle acceleration is bounded by the constant μg, where μ is the tyre/road friction coefficient and g is the gravitational acceleration. Thus, the vehicle's acceleration is subject to the following constraint:

$$\sqrt{a_x^2 + a_y^2} \le \mu g \tag{31}$$

In this study, constant speed is adopted, and thus the acceleration constraint can be reduced to

$$\left|a_y\right| \le \mu g \tag{32}$$

3. Vehicle's control and execution capability

As a mechanical system equipped with chassis active control systems, the vehicle's motion is limited by the vehicle's mechanical properties and electrical control system characteristics, which lead to the limits on the velocity control and the steering angle control. To make the vehicle's motion be smooth and safe, the vehicle's steering angle and their variations are constrained by

$$\delta_{fmin} \le \delta_{fk+i,t} \le \delta_{fmax} \tag{33}$$

$$\Delta\delta_{fmin} \le \Delta\delta_{fk+i,t} \le \Delta\delta_{fmax} \tag{34}$$

4. Tyre's slip angle limitation

The tyre's slip angle cannot be obtained directly from the vehicle's dynamic output as it has not been defined as a vehicle state, but it can be calculated with linearization based on the vehicle's output values (see eq.7 and eq.8).

$$C_{\alpha i} = \frac{\partial \alpha_i}{\partial X_s} \qquad i = f, r \tag{35}$$

$$D_{\alpha i} = \frac{\partial \alpha_i}{\partial u} \qquad i = f, r \tag{36}$$

Therefore, the output of the slip angle can be expressed by the vehicle's states

$$\alpha_i = C_{\alpha i} X_s + D_{\alpha i} u \qquad i = f, r \tag{37}$$

To avoid the tyre's large slip at some severe conditions, we use the following limits on the front and the rear tyre's slip angle to make sure the relationship between the tyre lateral force and the slip angle is limited to the linear range

$$\alpha_{\min} - \varepsilon \le \alpha_{f,k+i} \le \alpha_{\max} + \varepsilon \tag{38}$$

With the above constraints, the stability of the closed loop system can be maintained. Since the linear range of the relationship between lateral force and slip angle is maintained, the dynamic system is unable to enter into the possibly unstable region of the tyre characteristic.

In order to make the autonomous driving of the vehicles be natural and comfortable within the blended corridors obtained from environment risk elements and the vehicles' dynamic capabilities described above, the human-like autonomous driving problem can be described by the following optimization problem

$$\min_{\Delta U(t)} \quad J(\xi_t, \Delta U(t)) = \sum_{i=1}^{N_p} \left\| Y_{k+i,t} - Y_{k+i,t}^{ref} \right\|_Q^2 + \sum_{i=1}^{N_c-1} \left\| \Delta u_{k+i,t} \right\|_R^2 + \rho\varepsilon^2 \tag{39}$$

$$\begin{aligned} s.t.\ \ & X_d(k+i+1) = A_d X_d(k+i) + B_d u(k+i), i = 0,1,\dots,N_p - 1 \\ & Y_d(k+i+1) = C_d X_d(k+i), \qquad i = 0,1,\dots,N_p - 1 \\ & u_{min} \le u_{k+i,t} \le u_{max}, \qquad i = 0,1,\dots,N_c - 1 \\ & \Delta u_{min} \le \Delta u_{k+i,t} \le \Delta u_{max}, \qquad i = 0,1,\dots,N_c - 1 \\ & Y_{min} - \varepsilon \le Y_d(k+i+1) \le Y_{max} + \varepsilon, \quad i = 1,2\dots,N_p \\ & Yr_{min} \le Yr(k+i+1) \le Yr_{max}, \quad i = 1,2\dots,N_p \end{aligned} \tag{40}$$

It is noted that cost function of the vehicle dynamic controller can be designed according to the human driver's behaviour, which can be the minimum jerk of the vehicle, the minimum yaw angle deviation or the minimum lateral deviation of the vehicle. The constraint $Y_{min} - \varepsilon \le Y_d(k+i+1) \le Y_{max} + \varepsilon$ represents the limits of vehicle's states and other outputs that can be expressed by the vehicle's states, which include the vehicle's limits of lateral position, lateral acceleration, longitudinal speed, yaw rate, side slip angle and the tyres' slip angle. $Yr_{min} \le Yr(k+i+1) \le Yr_{max}$ denotes the risk-based corridor obtained from the human driving tests and the derived risk model expressed by the vehicle's states.

The optimal control problem describe by Eq.10 and Eq.11 can be transferred into a quadratic programming (QP) problem by the MPC solution procedure, in which way the optimisation vector ΔU, i.e. the sequence of the input increments $\Delta u(k), \Delta u(k+1), \dots, \Delta u(k+N_c-1)$ can be calculated. Therefore, transferring the cost function Eq. 39 and the constraints Eq. 40 into the standard QP problem, we get

$$\begin{aligned} & J(\xi_t, \Delta \boldsymbol{U}(t)) = \Delta \boldsymbol{U}(t)^{\mathrm{T}} \boldsymbol{H}_t \Delta \boldsymbol{U}(t) + \boldsymbol{G}_t \Delta \boldsymbol{U}(t)^{\mathrm{T}} \\ & \text{s.t.} \qquad \Delta \boldsymbol{U}_{min} \le \Delta \boldsymbol{U}_t \le \Delta \boldsymbol{U}_{max} \\ & \qquad \boldsymbol{U}_{min} \le \boldsymbol{A} \Delta \boldsymbol{U}_t + \boldsymbol{U}_t \le \boldsymbol{U}_{max} \end{aligned} \tag{40}$$

where $\boldsymbol{H}_t$ and $\boldsymbol{G}_t$ are the coefficients of the transferred QP problem. It is noted that only the first element of the control input series is adopted to the vehicle system at the current step, and then repeat this procedure at the next period.

6. Results and discussion

The traditional 2-dof nonlinear vehicle model is used in this study to represent the vehicle model illustrated in Fig.2. It has been shown that the bicycle vehicle model have agree well with the more complex 14 dof vehicle model, particularly for the non-severe scenarios (Na et al., 2015). Therefore, we used the 2 dof nonlinear vehicle model to represent the vehicle system that need to be controlled. The vehicle's parameters used in the simulation are shown in Table 2. The controller parameters used for the simulation are:

$$Q=\begin{bmatrix} W_4 & 0 & 0 & 0 \\ 0 & W_3 & 0 & 0 \\ 0 & 0 & W_2 & 0 \\ 0 & 0 & 0 & W_1 \end{bmatrix},\ T=0.05s,\ N_p=30,\ N_c=5,\ R=5\times10^3,\ \rho=1000,\ \mu=0.8$$

where $\begin{cases} W_1=2000, W_2=0, W_3=40, W_4=3000 & e_\psi>0.1 \\ W_1=3000, W_2=10, W_3=40, W_4=3000 & \left|e_y-boundary\right|\le 0.3 \\ W_1=1000, W_2=0, W_3=20, W_4=3000 & 0.3<\left|e_y-boundary\right|<0.5 \\ W_1=0, W_2=0, W_3=20, W_4=3000 & else \end{cases}$ and the boundary here represents the lateral offset boundary.

The steering angle has been constrained within the interval $-10^o \le \delta_f \le 10^o$, and the steering rate has been constrained to $-0.85^o \le \Delta\delta_f \le 0.85^o$. According to the tyre's properties (Wei and Olatunbosun, 2014), the controller implicitly limits the front tyre slip angle into its linear interval $[-3^o, 3^o]$.

The model parameters of the vehicle in the simulation are given in Table 2.

Table 2 Vehicle model parameters

Parameter	Description	Value
m	Total vehicle mass	1723 kg
I_z	Yaw moment of inertia	4175 kg
a	C.G. distance to front wheels	1.23 m
b	C.G. distance to rear wheels	1.47 m
C_f	Cornering stiffness of the front tyre	$\mathbf{6.69\times10^5}$ N/rad
C_r	Cornering stiffness of the rear tyre	$\mathbf{6.27\times10^5}$ N/rad
v	Velocity of the vehicle	10 m/s

To identify and estimate the predicted vehicle's trajectory within the risk-based corridor, four typical scenarios are defined and the acceptable lateral offsets within these scenarios are subject to the risk elements.

Scenario A: A J-turn curve is defined by involving two straight sections and one curve section with a curve radius of 50m, as shown in Figure 6. The J-turn curve starts from a straight section with a distance of 150m, followed by the 60m long arc curve and ended by a straight road section. Figure 6 shows the comparison between the centre line of the road and the vehicle's trajectory. Traditional path following motion control algorithms normally enable the vehicle to closely follow the centre line of the road if there is no obstacle or other dynamic risk element on the road. However, this leads to an anxiety for the drivers on the AVs as the steering manoeuvring action to follow the centre line of the curve is a little late compared to the natural

path taken by drivers. With the proposed vehicle motion controller, the vehicle follows the centre line of the road during the straight section and steers 20m ahead of the starting position of the curved section rather than exactly following the curve, after which the vehicle moves back to the centre of the road at the final straight road section.

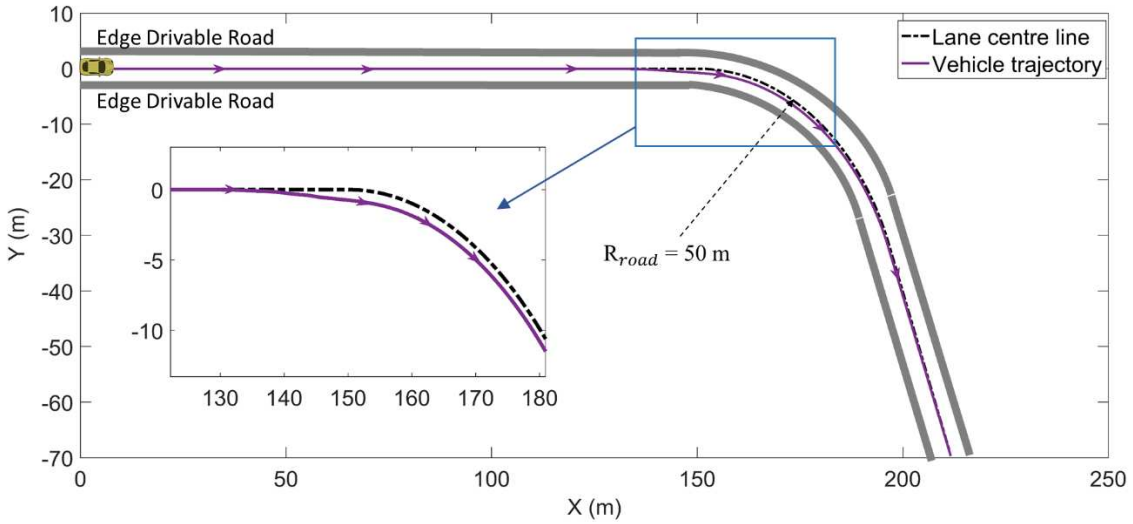

Figure 6 Simulation results for the J-turn scenario

Scenario B: For this scenario, a 300m straight road is defined by involving a short curve at the 100m position, as shown in Figure 7. The vehicle's velocity is set as 10km/h and the road width is 3.66m with only one lane. With the proposed vehicle motion controller, the vehicle is able to travel within the risk-based acceptable lateral offset. Due to traditional path planning and path following limitations mentioned above, we prefer to derive the risk-based corridor and make the AVs occupants have a comfortable and relaxed traveling experience for the drivers. Traditional path following vehicle controls normally choose the centre line of the road to follow and thus leads to a sharp cornering at the 100m position of this scenario. This behaviour of the AVs will make the drivers and the passengers feel strange and uncomfortable even though they do not affect the safety significantly. Different from the traditional path following solution schemes, the proposed controller enables the vehicle to have a nearly straight run at the straight road condition, and only have a slight steering variation at the sharp curve section area within the 300m straight road. It is noted that after the vehicle passes the short curve area it does not go back to the centre line of the road, which is different from the traditional path following control algorithms that force the vehicles to follow the centre line or the planed path. With the proposed control algorithm, the vehicle is allowed to travel in an acceptable lateral position and be parallel to the road centre line when it passes the sharp curve area, which aligns with the drivers' behaviour in practice.

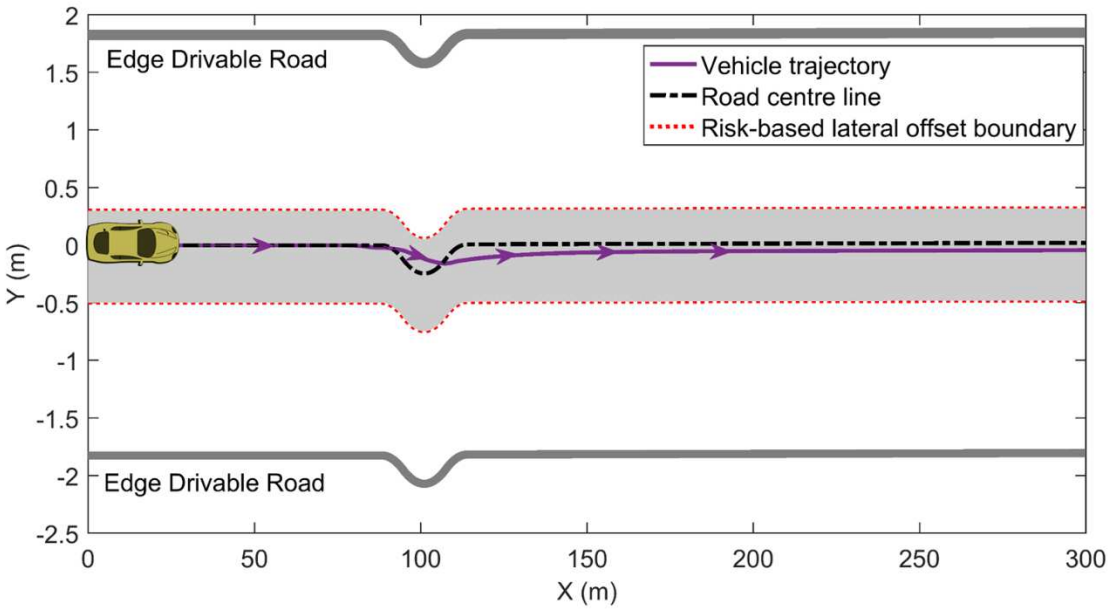

Figure 7 Simulation results for the straight road scenario with a short-curve

Scenario C: This scenario is defined by a double lane change section followed by a J-turn section and a straight road section, and the road has a width of 3.65 m, as shown in Figure 8. Note that the curved road sections within the full defined road have a radius of 170 m, which is the same as the radius of the experimental data. If the curved road is a left direction curve with a radius of 170 m, we consider it has an acceptable lateral offset of [-0.7327m, 0.4138m], while we consider the curved road to the right has an acceptable lateral offset of [-0.2342m, 0.7492m]. For the straight section of the road, we assume the acceptable lateral offset of the vehicle is [-0.2983m, 0.5071m]. Within the acceptable lateral offset, the safety of the autonomous driving can be guaranteed, which means the collision problems can be avoided. However, for some sharp curved sections, the drivers may feel very nervous when the AVs cannot steer in a timely fashion, i.e. following the centre line of the road. The vehicle's trajectory obtained with the proposed MPC algorithm enables the vehicle to steer early enough when it encounters a sharp curve section, see the highlight parts with the blue ellipses. When the vehicle returns to the straight road after having passed the curved road it keeps the vehicle heading direction the same as the road's direction but does not return to the centre line of the road, which aligns with the driving experience of the human driver.

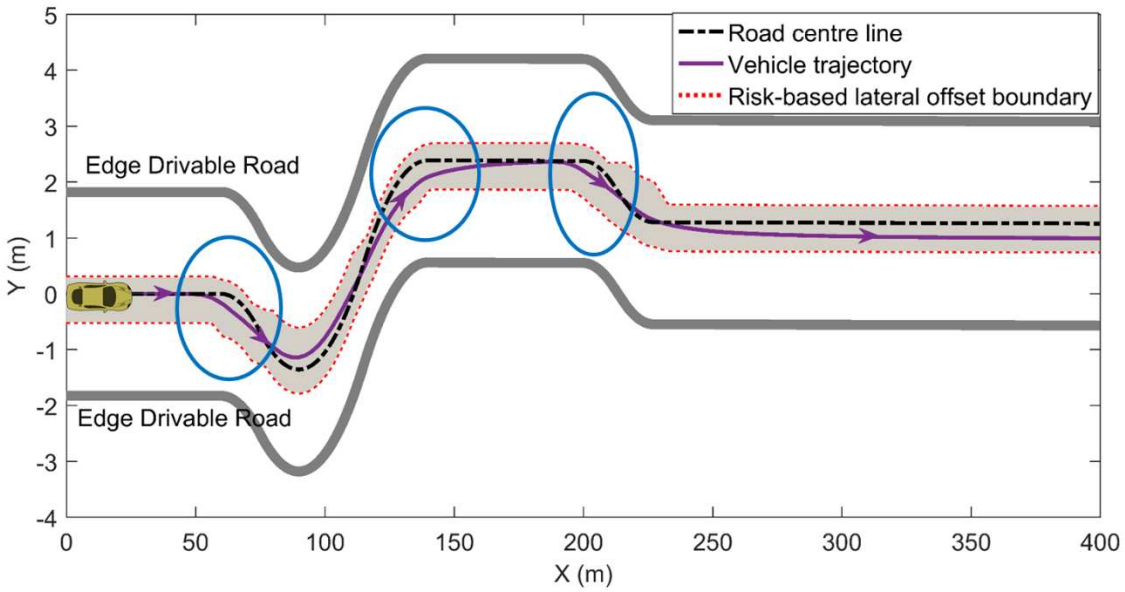

Figure 8 Simulation results for the Scenario C

Scenario D: For this scenario, the vehicle runs on a straight road with a parked car at the side of the road. Similar with the parked car setting in the driver simulator, 0.35 m width of the parking car is outside of the road and 1.45m of it is inside of the road, as shown in *Figure 9*. Considering the length of the host vehicle, the width of the obstacle length covering the parking car's length (4 m) is setting as 10 m. According to the statistical test data, the acceptable lateral offset at the parked car area is [0.99m, 1.97m], while the acceptable lateral offset for the straight road without obstacles is [-0.30m,0.50m]. The transition section between the two different acceptable lateral offsets is defined with the linearly varied curves at both the front and the rear of the parked car. The simulated vehicle trajectory within the derived lateral offset tolerance is shown in Figure 9. With the proposed controller and the derived risk-based corridor, the vehicle's trajectory can be limited in the corridor and has a smooth path. The vehicle starts to avoid the obstacle about 20m ahead, and slowly moves to the direction of the centre line when it passes the obstacle area. The simulation results also show that the vehicle tends to move in parallel with the road heading direction when it passes the obstacle and keeps traveling within the acceptable lateral offset. It can be seen that at this simple collision avoidance scenario, the proposed dynamic controller and the derived tolerance enables the vehicle to have a smooth and safe trajectory, and thus guarantees the comfortable experience without making the drivers of the AVs nervous.

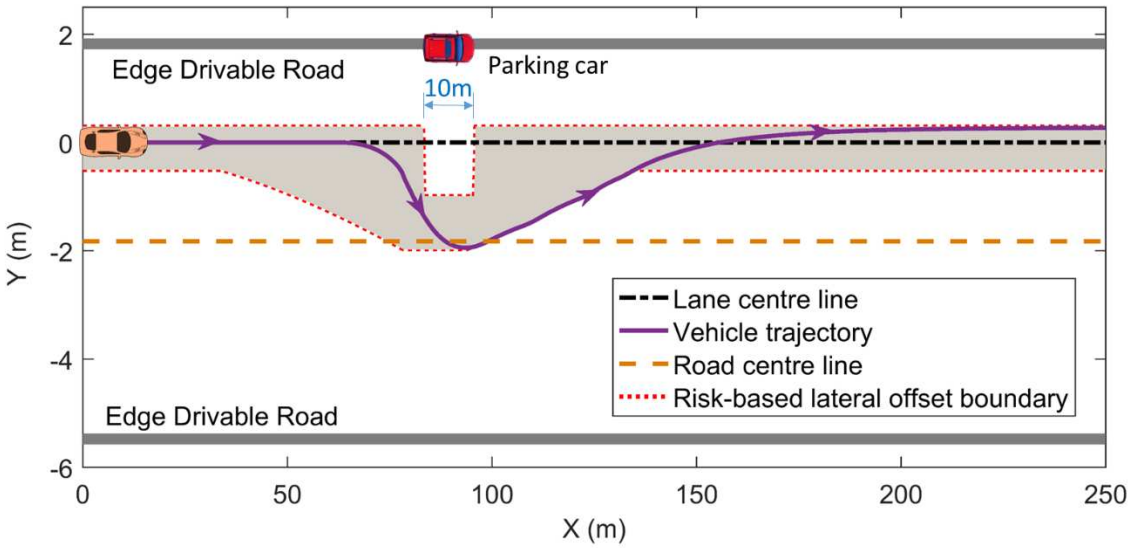

Figure 9 Simulation results for the scenario of static obstacle avoidance

Scenario E: This scenario is a straight road with a preceding moving vehicle with a lower speed (5m/s). To avoid the collision between the host vehicle and the dynamic risk element, i.e. preceding vehicle, we recreate the left and right boundaries of the lateral offset corridor based on the corridor for the straight road without obstacles. Both of the left and the right boundaries are built with a Gaussian Curve, and the preceding moving vehicle is accurately excluded from the corridor. The result illustrated in Figure 11 shows the vehicle is able to avoid the dynamic risk elements with the updated corridor, and a smooth trajectory has been obtained.

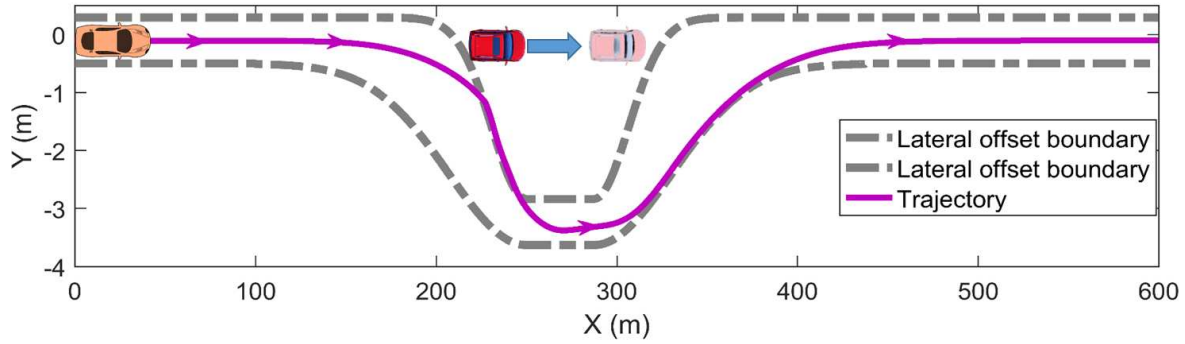

Figure 10 Simulation results for the scenario of dynamic obstacle avoidance

7. Conclusion

This study proposed a risk-corridor based vehicle motion control framework and some typical scenarios are simulated to verify the performance of the control method. The risk-based corridor was developed by the estimation of the acceptable lateral offset based on human driver testing within the driver simulator, while the vehicle dynamic corridor was defined by investigating the tyre/road interaction properties. 44 skilled drivers were tested for different road types and the drivers' behaviour as well as the vehicle's states such as positions, acceleration, speed, and yaw rate were collected and processed. The acceptable lateral offset tolerance were derived by processing the measured data of the drivers' manoeuvre actions.

With the derived lateral offset tolerance and the available vehicle dynamic constraints, a NMPC model has been developed by considering the comfort and sense of security and confidence of the drivers.

With the proposed controller and the vehicle dynamic model, four different typical scenarios were simulated and analysed. Rather than following the planned path, i.e. the centre line of the lane in this study, the proposed motion control model enables the vehicle to have a more comfortable and acceptable trajectory as expected by the drivers. Particularly, for the J-turn situation, the simulated results with the proposed controller shows the vehicle steers 2 s earlier from the straight road to the curved road than the road centre line, where following the path may lead to a sense of nervousness for the drivers. The simulated vehicle trajectory for sharp curve scenarios such as a double lane change shows the vehicle is able to have a smooth and stable motion within the derived corridor, while the road centre line path seems to be too sharp for the AVs and then it is not expected by the drivers. Collision avoidance in terms of avoiding the parking cars were also simulated to verify the feasibility of the controller, and the result shows the ego vehicle starts to avoid the parked car about 3s ahead and then gradually return to a position close to its original lateral position.

Acknowledgment

The work reported here is supported by the HumanDrive project, funded by the UK's Centre for Connected and Automated Vehicles (CCAV) and Innovate UK (Grant number TS/P012035/1). The authors gratefully acknowledge the contribution of Andrew Tomlinson, Anthony Horrobin, and Michael Daly for to the preparation of the simulated driving environment and preparation of the data for analysis.

References

Antonelli, G., Chiaverini, S., Fusco, G., 2007. A Fuzzy-Logic-Based Approach for Mobile Robot Path Tracking. *IEEE Transactions on Fuzzy Systems* 15(2), 211-221.

Berglund, T., Brodnik, A., Jonsson, H., Staffanson, M., Soderkvist, I., 2010. Planning Smooth and Obstacle-Avoiding B-Spline Paths for Autonomous Mining Vehicles. *IEEE Transactions on Automation Science and Engineering* 7(1), 167-172.

Boer, E.R., 2016. Satisficing Curve Negotiation: Explaining Drivers' Situated Lateral Position Variability. *IFAC-PapersOnLine* 49(19), 183-188.

Chu, K., Lee, M., Sunwoo, M., 2012. Local Path Planning for Off-Road Autonomous Driving With Avoidance of Static Obstacles. *IEEE Transactions on Intelligent Transportation Systems* 13(4), 1599-1616.

Du, H., Zhang, N., Naghdy, F., 2011. Velocity-dependent robust control for improving vehicle lateral dynamics. *Transportation Research Part C: Emerging Technologies* 19(3), 454-468.

Ferguson, D., Howard, T.M., Likhachev, M., 2008. Motion planning in urban environments: Part I, *2008 IEEE/RSJ International Conference on Intelligent Robots and Systems*, pp. 1063-1069.

González, D., Pérez, J., Lattarulo, R., Milanés, V., Nashashibi, F., 2014. Continuous curvature planning with obstacle avoidance capabilities in urban scenarios, *17th International IEEE Conference on Intelligent Transportation Systems (ITSC)*, pp. 1430-1435.

González, D., Pérez, J., Milanés, V., Nashashibi, F., 2016. A Review of Motion Planning Techniques for Automated Vehicles. *IEEE Transactions on Intelligent Transportation Systems* 17(4), 1135-1145.

Gu, T., Dolan, J.M., Lee, J., 2016. Human-like planning of swerve maneuvers for autonomous vehicles, *2016 IEEE Intelligent Vehicles Symposium (IV)*, pp. 716-721.

Hu, C., Jing, H., Wang, R., Yan, F., Chadli, M., 2016a. Robust H∞ output-feedback control for path following of autonomous ground vehicles. *Mechanical Systems and Signal Processing* 70-71, 414-427.
Hu, C., Wang, R., Yan, F., 2016b. Integral Sliding Mode-Based Composite Nonlinear Feedback Control for Path Following of Four-Wheel Independently Actuated Autonomous Vehicles. *IEEE Transactions on Transportation Electrification* 2(2), 221-230.
Jeong hwan, J., Cowlagi, R.V., Peters, S.C., Karaman, S., Frazzoli, E., Tsiotras, P., Iagnemma, K., 2013. Optimal motion planning with the half-car dynamical model for autonomous high-speed driving, *2013 American Control Conference*, pp. 188-193.
Ji, J., Khajepour, A., Melek, W.W., Huang, Y., 2017. Path Planning and Tracking for Vehicle Collision Avoidance Based on Model Predictive Control With Multiconstraints. *IEEE Transactions on Vehicular Technology* 66(2), 952-964.
Kala, R., Warwick, K., 2013. Multi-Level Planning for Semi-autonomous Vehicles in Traffic Scenarios Based on Separation Maximization. *Journal of Intelligent & Robotic Systems* 72(3), 559-590.
Karaman, S., Walter, M.R., Perez, A., Frazzoli, E., Teller, S., 2011. Anytime Motion Planning using the RRT*, *2011 IEEE International Conference on Robotics and Automation*, pp. 1478-1483.
Kuwata, Y., Teo, J., Fiore, G., Karaman, S., Frazzoli, E., How, J.P., 2009. Real-Time Motion Planning With Applications to Autonomous Urban Driving. *IEEE Transactions on Control Systems Technology* 17(5), 1105-1118.
Na, S., Jang, J., Kim, K., Yoo, W., 2015. Dynamic vehicle model for handling performance using experimental data. *Advances in Mechanical Engineering* 7(11), 1687814015618126.
Ntousakis, I.A., Nikolos, I.K., Papageorgiou, M., 2016. Optimal vehicle trajectory planning in the context of cooperative merging on highways. *Transportation Research Part C: Emerging Technologies* 71, 464-488.
Rashid, A.T., Ali, A.A., Frasca, M., Fortuna, L., 2013. Path planning with obstacle avoidance based on visibility binary tree algorithm. *Robotics and Autonomous Systems* 61(12), 1440-1449.
Wei, C., Olatunbosun, O.A., 2014. Transient dynamic behaviour of finite element tire traversing obstacles with different heights. *Journal of Terramechanics* 56, 1-16.
Wei, C., Olatunbosun, O.A., 2016. The effects of tyre material and structure properties on relaxation length using finite element method. *Materials & Design* 102, 14-20.
Wei, C., Olatunbosun, O.A., Behroozi, M., 2016. Simulation of tyre rolling resistance generated on uneven road. *International Journal of Vehicle Design* 70(2), 113-136.
Wei, C., Olatunbosun, O.A., Yang, X., 2017. A finite-element-based approach to characterising FTire model for extended range of operation conditions. *Vehicle System Dynamics* 55(3), 295-312.
Wenda, X., Junqing, W., Dolan, J.M., Huijing, Z., Hongbin, Z., 2012. A real-time motion planner with trajectory optimization for autonomous vehicles, *2012 IEEE International Conference on Robotics and Automation*, pp. 2061-2067.
Wu, C., Peng, L., Huang, Z., Zhong, M., Chu, D., 2014. A method of vehicle motion prediction and collision risk assessment with a simulated vehicular cyber physical system. *Transportation Research Part C: Emerging Technologies* 47, 179-191.
Ziegler, J., Bender, P., Dang, T., Stiller, C., 2014. Trajectory planning for Bertha — A local, continuous method, *2014 IEEE Intelligent Vehicles Symposium Proceedings*, pp. 450-457.